Mycosphere 9(6): 1235–1255 (2018) www.mycosphere.org ISSN 2077 7019
Article
Doi 10.5943/mycosphere/9/6/12

Phylogenetic relationship and evolution of *Neodidymelliopsis* isolates collected from Iran

Soleimani P[1], Soleimani MJ[1*] and Hosseini S[2]

[1] *Department of Plant Protection, College of Agriculture, Bu-Ali Sina University, Hamedan, Iran*
[2] *Department of Plant Protection, College of Agriculture, Vali-e-Asr University of Rafsanjan, Rafsanjan, Iran*

Soleimani P, Soleimani MJ, Hosseini S 2018 – Phylogenetic relationship and evolution of *Neodidymelliopsis* isolates collected from Iran. Mycosphere 9(6), 1235–1255, Doi 10.5943/mycosphere/9/6/12

Abstract

Several isolates of the novel genus *Neodidymelliopsis* have been recently found in Iranian citrus orchards with severe dieback symptoms. *Neodidymelliopsis* belongs to Didymellaceae, an important family of Pleosporales, Dothideomycetes. None of the few studies on molecular dating of Ascomycetes have resolved the divergence time of genera in Didymellaceae. Motivated by this fact, we consider the reliable age of a fossil related to extant species of *Aigilalus*, the estimated mean crown age of Dothideomycetes from other studies as a secondary calibration, also the second fossil which represent common ancestor of Capnodiales to calibrate the reconstructed tree. Our dating analysis is based on four genetic regions of 91 taxa from Capnodiales and Pleosporales, using BEAST analysis. The selected taxa of Pleosporales belong to Aigialaceae and Didymellaceae; including three newly discovered *Neodidymelliopsis* sp. isolates and one isolate of *Didymella* sp. from Iran. Our dating analyses suggest that Didymellaceae diverged from Aigialaceae in the Cretaceous, and initial divergence of Didymellaceae happened in the late Eocene followed by two divergences in the late Oligocene and several splits in the Miocene. Furthermore, the results suggest that the Iranian isolates of *Neodidymelliopsis* sp. and *Didymella* sp. diverged from other *Neodidymelliopsis* and *Didymella* isolates in the Pliocene and the late Miocene, respectively.

Key words – Didymellaceae – Divergence time – Fossil – Pleosporales – Secondary calibration

Introduction

Coelomycetes are a form-class of fungi which produce their conidia and conidiophore within the cavity like pycnidia (globose to pyriform conidiomata from which the conidia arise throughout an apical opening) or sporocarp (de Gruyter et al. 2009, Chen et al. 2015). This form-class of fungi consists of numerous endophytic, pathogenic or saprobic fungi in terrestrial and marine ecosystems, or in plants and animals (Dai et al. 2014, Hyde et al. 2014, Wijayawardene et al. 2016).

Coelomycetous fungi has been recently assigned to different phylogenetic groups, e.g. Dothideomycetes, Leotiomycetes and Sordariomycetes (Wijayawardene et al. 2016, 2017). Dothideomycetes is well-known class of Ascomycota (Wijayawardene et al. 2017, 2018), while Pleosporales contains a quarter of the class (Kirk et al. 2008), with Didymellaceae as the largest family in this order. Didymellaceae encompasses more than 5,400 taxa in MycoBank (Crous et al. 2004, Crous & Groenewald 2017, Hashimoto et al. 2017). In the recent revision of Didymellaceae,

Submitted 25 January 2018, Accepted 8 August 2018, Published 25 December 2018
Corresponding Author: Parisa Soleimani – e-mail – soleimani302p@yahoo.com

26 genera belong to this family have been reported (Chen et al. 2015, 2017, Valenzuela-Lopez et al. 2018). Members of this family are pathogenic on a wide range of host plants, which mainly cause leaf and stem lesions and some are of quarantine significance (Aveskamp et al. 2008, Boehm et al. 2009, Chen et al. 2017). Recently, some isolates of the novel genus *Neodidymelliopsis* and *Didymella* have been found on the citrus trees with severe dieback symptoms in Iran. This motivated our research to find out the divergence time of the selected isolates of Didymellaceae, particularly, isolates of *Neodidymelliopsis* sp. and *Didymella* collected from southern parts of Iran by comparing their nucleotide sequences. To achieve this aim, we adopted a molecular dating approach based on the molecular clock hypothesis (MCH), proposed by Zuckerkandl & Pauling (1965).

Molecular dating combines information from the fossils, recorded events, geological events and those achieved from data analyses to estimate the age of clades in a phylogenetic tree (Rutschmann 2006, Ho & Duchene 2014). It is also possible to use the estimated age of a node from previous studies to calibrate the molecular clock in a new study, as a secondary calibration (dos Reis et al. 2015). Recently, several molecular dating studies have tried to estimate the age of fungi based on the available fossils (Vijaykrishna et al. 2006, Beimforde et al. 2014, Hongsanan et al. 2016, Zhao et al. 2016, Hyde et al. 2017, Liu et al. 2017). However, lack of the reliable fossils is a limited factor in molecular dating studies, which could face even a bigger challenge when the microscopic structure of fungi is unknown (Prieto & Wedin 2013).

Here, we first constructed a phylogenetic tree based on four multi-gene datasets including the four sequenced isolates and some taxa of Didymellaceae obtained from the National Center for Biotechnology Information (NCBI) databases. We performed the dating analysis which updated the age of Dothideomycetes, Pleosporales and gave the first estimation of the divergence time of Didymellaceae genera.

Materials & Methods

Sample collection, DNA extraction and sequencing

We collected citrus samples with dieback, blight of vigorously growing shoots symptoms, from citrus orchards in three southern provinces of Iran (Kerman, Hormozgan and Khuzestan). Pathogen isolation and inoculum preparation were performed according to the methods described by Taylor & Hyde (2003). Pure cultures were obtained by single spore isolation methods (Chomnunti et al. 2014). Four isolates were deposited at Centraalbureau voor Schimmelcultures (CBS) Fungal Biodiversity Center in the Netherlands and Iranian Fungal Culture Collection (IRAN.C) at the Iranian Research Institute of Plant Protection (Supplementary table 1).

The genomic DNA was extracted using Doyle & Doyle (1987) protocol from the fungal mycelium produced in Potato Dextrose Agar (PDA) media at 25−27°C for 4 weeks. We amplified four genomic regions including partial large subunit nuclear rDNA (28S, LSU), internal transcribed spacer regions 1 & 2 and intervening 5.8S nrDNA (ITS), partial RNA polymerase II second largest subunit (RPB2) and partial beta-tubulin (TUB2) region using special primers (Table 1), as it was described by Chen et al. (2015). PCR products were visualized under UV light after electrophoresis in a 1.0 % (w/v) agarose gel containing 0.1 ug/mL ethidium bromide in 1 × TAE buffer. Sanger sequencing was performed by Macrogen Company (Seoul, Korea), and results were submitted to NCBI (Supplementary table 1).

Sequence alignment and phylogenetic analysis

To determine the phylogenetic relationship of the selected Iranian isolates with the other available taxa, we considered LSU, RPB2, TUB2 and ITS genomic regions in all 26 accepted Didymellaceae genera, as mentioned by Valenzuela-Lopez et al. (2018). In addition, we used seven *Aigialus* and Capnodiales isolates; according to Beimforde et al. (2014), Phukhamsakda et al. (2016) as the out-group. The selected strains and their accession numbers were listed in Supplementary table 2. The genetic regions were separately aligned by MAFFT v.7 (Katoh &

Standley 2013). We checked the alignment visually and adjusted it manually in Mesquite v.3.04 (Maddison & Maddison 2015). The alignments were concatenated by SequenceMatrix program (Vaidya et al. 2011). Linux version of IQ-tree tool v.1.6 (Nguyen et al. 2014) was used to reconstruct the phylogenetic trees and find the best substitution model. We assessed the reliability of the reconstructed branches by Bootstrap analyses on 1000 replicates, and visualized trees in FigTree v.1.4.2.

Table 1 Primers used in this study.

Regions	Primer pairs	Reference
ITS	V9G/ITS4	White et al. (1990), de Hoog & Gerrits van den Ende (1998)
RPB2	RPB2-5F2/fRPB2-7cR	Liu et al. (1999), Sung et al. (2007)
LSU	LR0R/LR7	Vilgalys & Hester (1990), Rehner & Samuels (1994)
TUB2	Btub2Fd/Btub4Rd	Woudenberg et al. (2009)

Node Calibrations

To calibrate the nodes, we took advantage of the age of the reliable fossils and the estimated mean crown age of Dothideomycetes. We compared three calibration scenarios, based on the minimum age of reliable fossils from the literature and the secondary calibration. The calibration based on the age of a node estimated in other study is referred to as secondary calibration (Ho & Duchene 2014, dos Reis et al. 2015). In all cases, we considered Pleosporales as a monophyletic group.

In scenario I, we used a fossil of *Margaretbarromyces dictyosporus* (Fossil I) which belongs to Pleosporales with the age of 35−55 Mya (Mindell et al. 2007, Berbee & Taylor 2010, Phukhamsakda et al. 2016). Since morphologically this fungus resembles *Aigialus* belonging to Aigialaceae, Pleosporales (Phukhamsakda et al. 2016), we assigned the estimated age of the fossil to the node of *Aigialus* cluster (AIG). To demonstrate the uncertainty of the fossil age we represented it by a lognormal distribution with an offset (minimum bound), because we did not have any information about the maximum bound of the age (Ho & Philips 2009), with the mean of TMRCA (the most recent common ancestor) of *Aigialus* = 35, SD = 3.5, offset = 34, giving 95% credibility interval (CI) of 58.

In scenario II, we used two fossils *viz*. *M. dictyosporus* to calibrate AIG node and a Metacapnodiaceae fossil (~100−113 Mya, Schmidt et al. 2014) to calibrate the crown node of Capnodiales (CAP). In this scenario, we used the same setting as scenario I for *M. dictyosporus* fossil, while used a lognormal distribution (mean = 100, SD = 4.5, offset = 99, CI = 120) for the Metacapnodiaceae fossil.

For scenario III, besides the age of two pre-mentioned fossils, we considered the estimated mean crown age of Dothideomycetes (107−459 Mya) on the root of the tree estimated by Gueidan et al. (2011), Prieto & Wedin (2013), Beimforde et al. (2014), Pérez-Ortega et al. (2016), Phukhamsakda et al. (2016) as a secondary calibration. We preferred a uniform distribution (with maximum of 457 and minimum of 107) for the secondary calibration, as simulation studies (Schenk 2016) reported that the normal prior distribution results in larger errors, compared to uniform distribution in the secondary calibrations. Fig. 1 illustrates the posterior probability density distribution of the three calibration points.

Molecular dating

We used the BEAST v1.8.2 package (Drummond et al. 2012) for the molecular dating analysis. For this analysis, we used an uncorrelated lognormal relaxed clock model (UCLD) and the simplest model, Yule process (Drummond & Bouckaert 2014). GTR substitution model, 4 rate categories were used based on the suggestion from the model finder of IQ-tree. Since Gamma and invariable sites have a mutual effect (Drummond & Bouckaert 2014, Moran et al. 2015), applying both on a model is not biologically meaningful (Jia et al. 2014). Hence, we excluded invariable sites from the substitution model and set up the mean rate to the continuous-time Markov chains

model (CTMCs), recommended by Ferreira & Suchard (2008). We performed three MCMC analyses of 400 million generations, with sampling every 10000 steps. The results were evaluated by Tracer v1.6. The effective sample size (ESS) values of parameters were checked and improved to be more than 200 (Drummond & Bouckaert 2014). The resulted log and tree files were combined using LogCombiner1.8.0. Finally, we summarized the BEAST results by TreeAnnotator v1.4.7 with a burn-in of 10% and displayed them in FigTree v.1.4.2.

To compare different scenarios, we estimated the marginal likelihood (MLE) using path sampling (PS) and stepping stone sampling (SS), implemented in BEAST.

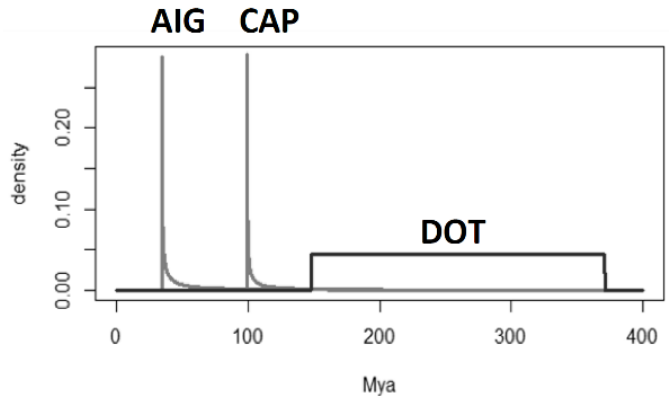

Figure 1 – The plot posterior probability density distribution of used calibration points. The AIG, CAP and DOT curves show the probability of used calibration points assigned to MRCA of *Aigialus*, Capnodiales and Dothideomycetes nodes respectively.

Results

Phylogenetic analysis

The concatenated file produced by SequenceMatrix, adjusted in Mesquite, contained 91 taxa with 2,864 characters. Fig. 2 summarizes the results of our phylogenetic analyses; the four sequenced taxa have been marked with black diamonds. IR67 isolate clustered with *Didymella glomerata* CBS 528.66, while IR10, IR26 and IR14 isolates clustered with *Neodidymelliopsis longicolla* CBS 382.96 with high bootstrap supports (99-100).

Molecular dating analysis

Comparing different scenarios

To compare different scenarios, we estimated the marginal likelihood (Table 2) which was slightly higher in scenario III, compared with the other scenarios.

Divergence time

The constructed trees in all scenarios (Fig. 4, Supplementary figs 1, 2) were consistent to the best tree built by IQ-tree (Fig. 2). Most of the estimated mean of nodes are supported by a strong posterior probability. The crown and stem age of all nodes in scenario III are considered as the best scenario (see discussion, Table 3). Pleosporales diverged from Capnodiales at ~144.5 (107−202.9) Mya. Within Pleosporales, Didymellaceae diverged from Aigialaceae at ~86.7 (53.9−155.4) Mya. The mean age of the earliest split in Didymellaceae (*Neoascochyta* from other genera) is ~35.7 (18.4−63.5) Mya. The newest split of *Briansuttonomyces* and *Pseudoascochyta* from other genera in Didymellaceae occurred at ~6.3 (2−13.2) Mya. Iranian isolates of *Neodidymelliopsis* sp. and *Didymella* sp. diverged from other *Neodidymelliopsis* and *Didymella* isolates at ~3.1 (0.9−6.9) and

~8.6 (3.5−16.8) Mya, respectively (Fig. 4). Time charts of the nodes based on the estimated crown and stem ages in this student can be seen in Supplementary tables 4, 5.

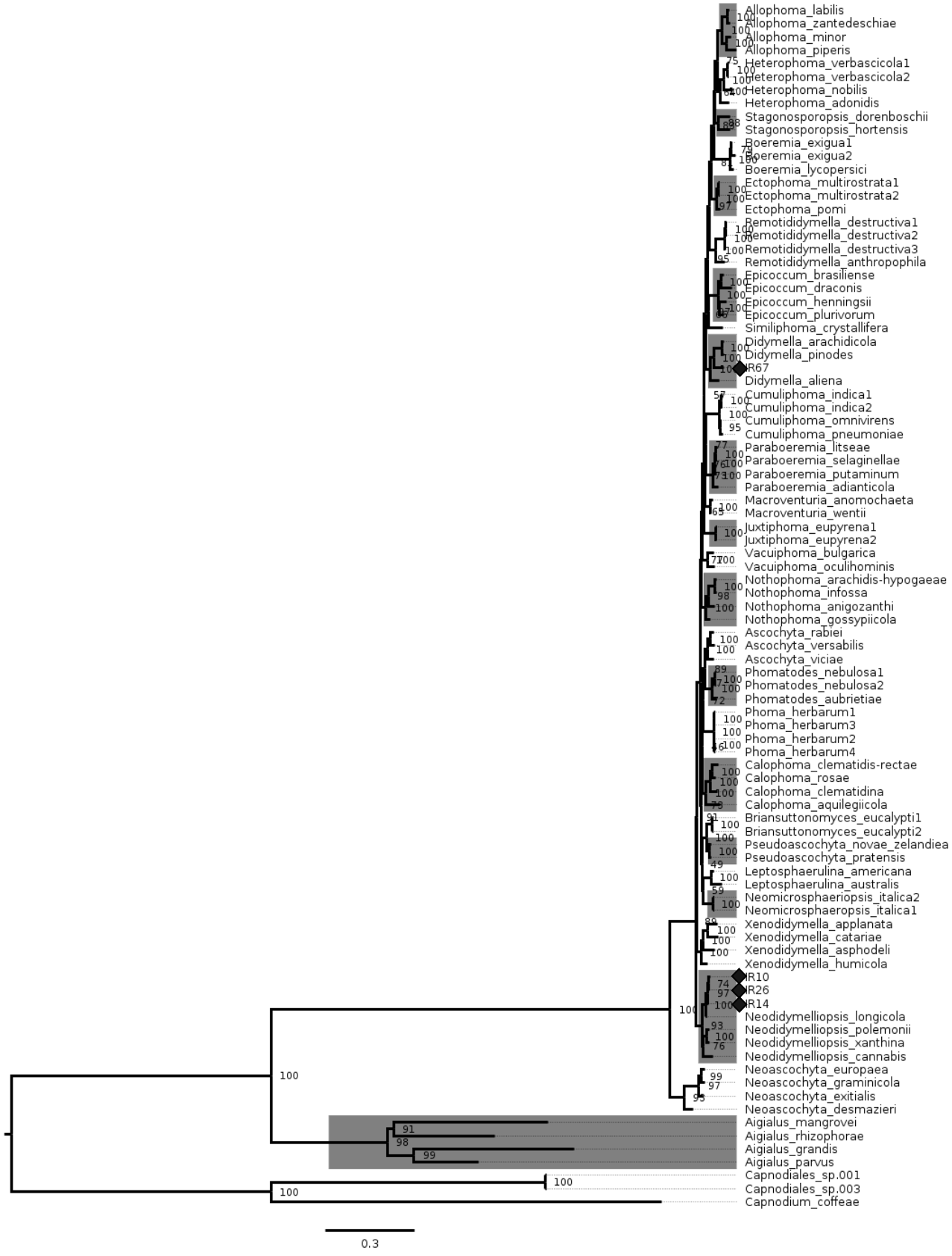

Figure 2 – The result of phylogenetic analyses. Bootstrap values are shown next to the nodes and the Iranian isolates are marked with black diamonds.

Table 2 The estimated marginal likelihood in different models.

Scenario	Log (Marginal likelihood) with SS	Log (Marginal likelihood) with PS
I	-26647.1	-26647.4
II	-26646.0	-26645.3
III	-26643.7	-26643.6

The comparison between the 95% HPD (Highest Posterior Density) of four main nodes, MRCA of Dothideomycetes (DOT), Didymellaceae (DID), Pleosporales (PLE) and *Neodidymelliopsis* (NEO) nodes showed that the intervals of the defined scenarios are overlapped (Fig. 3). In Table 3, estimated age of crown nodes and interval of 95% HPD are listed.

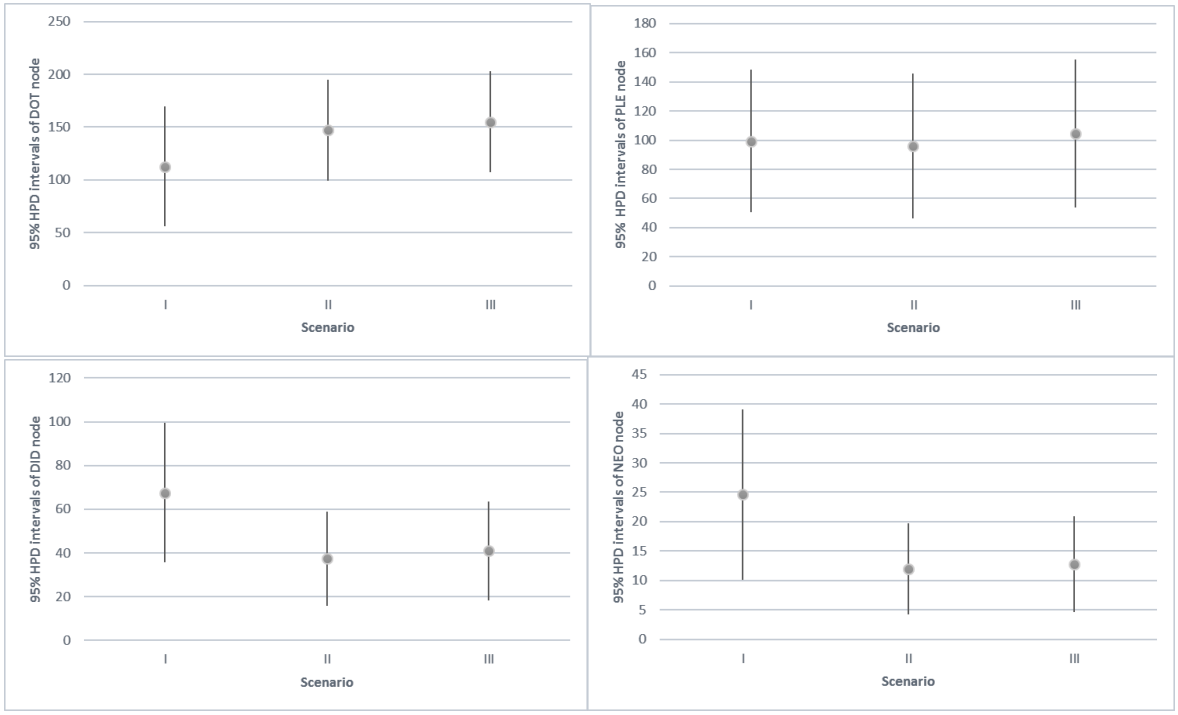

Figure 3 – Comparison means and interval of estimated age for MRCA of Dothideomycetes (DOT), Didymellaceae (DID), Pleosporales (PLE) and *Neodidymelliopsis* (NEO).

Table 3 The estimated divergence time of the crown nodes of Dothideomycetes in the three defined scenarios. Last column presents the estimated stem age in scenario III (the best scenario). Mean and 95% HPD intervals of each node have been presented in square brackets in millions of years (Mya).

Taxa (Node name)	Scenario I (1 Fossil)	Scenario II (2 Fossils)	Scenario III (2 Fossils and 2nd calibration)	
	Crown node	Crown node	Crown node	Stem node
Capnodiales (CAP)	44.4[17.6-82.5]	99[99-100.1]	99[99-100.1]	144.5[107-202.9]
Pleosporales (PLE)	92.4[50.5-148.1]	80.2[46.3-145.7]	86.7[53.9-155.4]	144.5[107-202.9]
Aigialus (AIG)	34.1[34-38]	34.1[34-59.4]	34.1[34-64.4]	86.7[53.9-155.4]
Didymellaceae (DID)	63[35.6-99.4]	32.5[16-59]	35.7[18.4-63.5]	86.7[53.9-155.4]
Neodidymelliopsis (NEO)	21.9[10.1-39.1]	10.1[4.3-19.7]	10.9[4.7-20.87]	27.3[15.9-45.8]
Iranian *Neodidymelliopsis* (IRneo)	3.3[1.2-6.3]	1.5[0.4-3.3]	1.6[0.5-3.5]	3.1[0.9-6.9]

Table 3 Continued.

Taxa (Node name)	Scenario I (1 Fossil)	Scenario II (2 Fossils)	Scenario III (2 Fossils and 2nd calibration)	
	Crown node	Crown node	Crown node	Stem node
Allophoma (ALL)	14.2[7.2-23.3]	7.4[3.6-13.5]	7.7[3.8-13.8]	10.8[5.8-18.7]
Heterophoma (HET)	15.1[7.5-24.6]	7.7[3.6-13.9]	8.02[3.8-14.3]	10.8[5.8-18.7]
Stagonosporopsis (STA)	15.1[7-25.6]	8[3-15]	8.3[3.4-15.6]	12.6[6.2-22]
Boeremia (BOE)	9.1[3.9-16.5]	4.3[1.4-8.9]	4.5[1.6-9.3]	13.8[7.5-24]
Ectophoma (ECT)	8.3[2.9-16.9]	3.9[0.9-9.6]	4.1[1-9.9]	15.3[8.5-27]
Remotididymella (REM)	16.1[7.5-27.8]	8.7[3.1-17.3]	9.1[3.3-17.8]	16.5[9.3-29.2]
Epicoccum (EPI)	15.6[7.6-26.3]	8.3[3.7-15.6]	8.6[4-16.2]	15.4[7.9-27.5]
Similiphoma (SIM)	26.7[14.6-42.8]	15[7.6-26.9]	15.4[7.9-27.5]	16.5[9.3-29.2]
Didymella (DIM)	21.4[10.9-35.4]	12.6[5.8-23.2]	13.1[6.05-23.8]	17.1[9.3-29.6]
Cumuliphoma (CUM)	7.6[3.2-13.9]	3.6[1.2-7.6]	3.7[1.3-8]	14.9[7.5-26.2]
Paraboeremia (PAR)	11.5[4.9-21.3]	5.6[1.9-11.7]	5.8[2.1-12.1]	14.9[7.5-26.2]
Macroventuria (MAC)	5.4[1.5-11.6]	2.7[0.5-7.5]	2.9[0.5-7.8]	16.9[8.6-26.2]
Juxtiphoma (JUX)	2.4[0.6-5.3]	1.1[0.2-3.1]	1.1[0.2-3.3]	19[10.6-32.4]
Vacuiphoma (VAC)	16.6[6.2-31.1]	9.3[2.5-19.6]	9.9[2.7-20.4]	21.6[12.7-35.3]
Nothophoma (NOT)	21.5[9.9-38.5]	10.2[4.2-19.3]	10.7[4.4-20]	17.1[9.3-29.6]
Ascochyta (ASC)	14.7[6.9-25.3]	7.5[3.1-13.8]	8[3.5-14.5]	11[5.7-19.2]
Phomatodes (PHT)	7.7[2.7-14.9]	3.7[1-8.2]	3.9[1.1-8.6]	11[5.7-19.2]
Phoma (PHO)	1.2[0.3-2.8]	0.6[0.1-1.6]	0.6[0.1-1.7]	16.5[9-27.7]
Calophoma (CAL)	23.1[11.5-38.1]	12.3[5.6-21.8]	13.1[6.3-23.1]	18.5[10.2-30.7]
Briansuttonomyces (BRI)	0.1[0-0.9]	0.1[0-0.7]	0.1[0-0.7]	6.3[2-13.2]
Pseudoascochyta (PSE)	3.2[1-6.6]	1.5[0.3-3.9]	1.6[0.3-4.1]	6.3[2-13.2]
Leptosphaerulina (LEP)	14.3[5-27.6]	6.7[1.7-14.8]	7.2[2-15.9]	20.2[11.7-33.7]
Neomicrosphaeropsis (NEM)	0.6[0.04-2]	0.3[0.01-1.1]	0.3[0.01-1.1]	13.3[6.9-22.5]
Xenodidymella (XEN)	30.3[15.2-50.7]	14.7[6.7-27.4]	16[7.4-29.1]	25.8[15-42.7]
Neoascochyta (NEA)	31.2[13.8-54.6]	13.5[4-43.3]	15.2[5.3-31.7]	35.7[18.4-63.5]

Discussion

In recent decade, there has been an increasing interest in molecular dating of species as an effective way of studying molecular evolution (Ho & Philips 2009, dos Reis et al. 2015). A few molecular dating studies have tried to estimate the divergence time of Ascomycetes and their orders (e.g. Beimforde et al. 2014, Hongsanan et al. 2016, Zhao et al. 2016, Hyde et al. 2017, Liu et al. 2017). In this study, we focused on divergence time of Didymellaceae genera for the first time, with added three *Neodidymelliopsis* and one *Didymella* isolates, collected from three provinces of Iran.

The phylogenetic tree indicated that Iranian *Didymella* isolate clustered with *D. glomerata* with a high bootstrap support, this result is also supported by morphological identification (data not published). Newly isolates of *Neodidymelliopsis* obtained in this study are closely related to *N. longicolla* with high bootstrap support. Morphological features of these new fungal isolates collected from citrus in southern Iran, confirmed that they share *Neodidymelliopsis* properties by having possessed pycnidial conidiomata and phialidic conidiogenesis, with hyaline, ampulliform, thin-walled conidiogenous cells, non or 1-septate, smooth-walled, hyaline to pale brown conidia. Characterization of conidiomata, conidia and conidiogenous cells of the isolates were in consistent with the description of *Neodidymelliopsis* reported by Chen et al. (2015). Since the main aim of this study was to focus on the molecular dating of these isolates, more morphological and pathological studies could be subject of further future works.

In the reconstructed phylogenetic tree (Fig. 1), the taxa related to Didymellaceae formed a sister group to the four selected *Aigialus* species within Pleosporales. The Capnodiales can be considered as an out-group, as they diverged from other taxa of Pleosporales. All the nodes of Didymellaceae, Aigialaceae, Pleosporales, and Capnodiales, where the main clusters have been

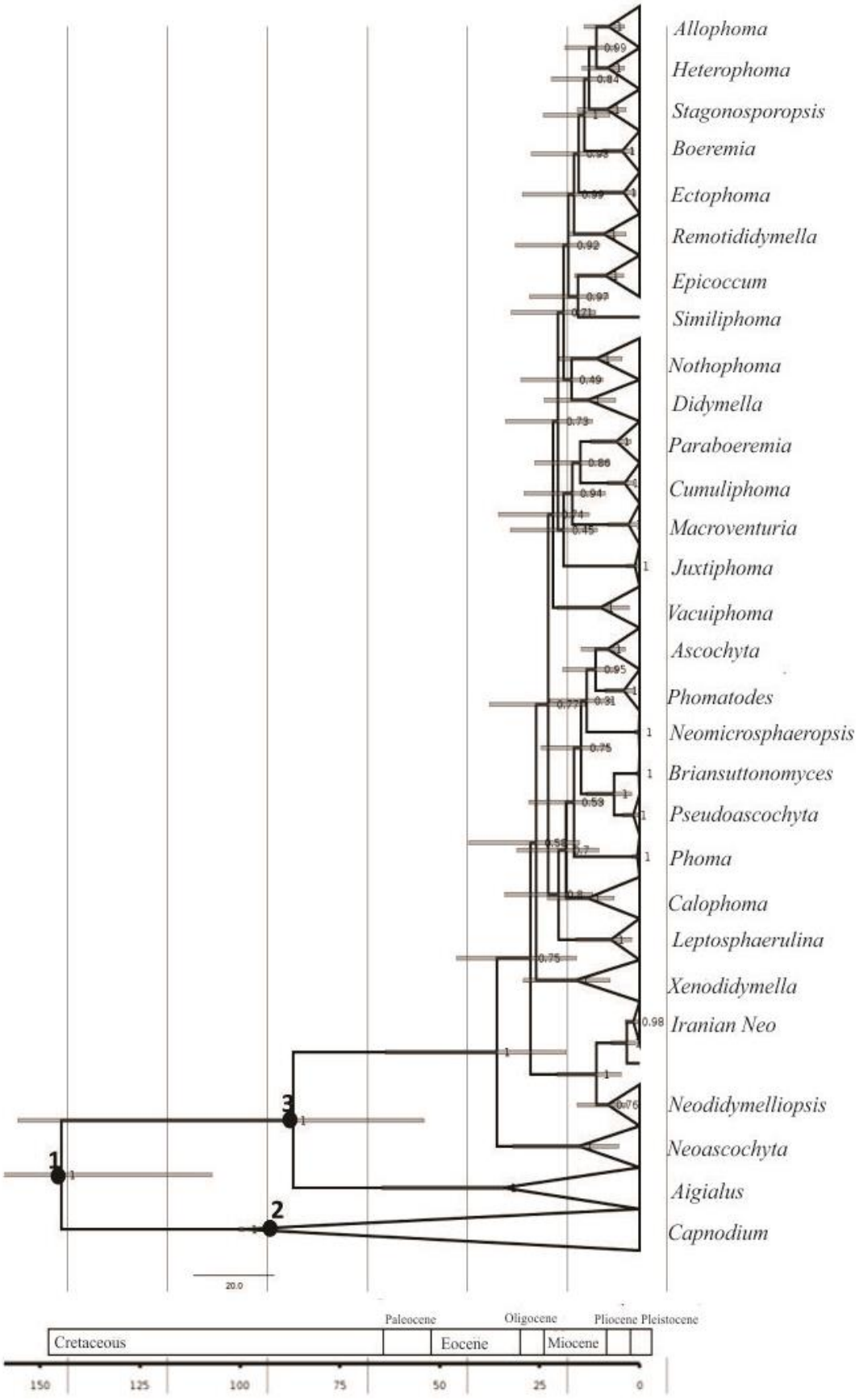

Figure 4 – Dated phylogenetic tree of scenario III. The numbers next to the nodes indicate the posterior probability values. The gray horizontal bars show the 95% HPD intervals of the node ages. Nodes 1-3 are the calibration points (MRCA of Dothideomycetes, Capnodiales and *Aigialus* respectively).

branched are well-supported (Fig. 1). These results are congruence with the previous studies (Aveskamp et al. 2010, Hyde et al. 2016, Phukhamsakda et al. 2016, Chen et al. 2017, Valenzuela-Lopez et al. 2018). In molecular dating analyses, the means of estimated ages in scenario I (with one fossil) are lower than other scenarios, with widest interval of 95% HPD (Supplementary table 3). Although the intervals of 95% HPD and the estimated age of the nodes in scenario II and III are very similar, we consider scenario III as the best scenario due to the higher marginal likelihood.

Base on strains and parameters used in this study, we conclude that the earliest divergence in Didymellaceae is in the late Eocene when *Neoascochyta* diverged from other genera in Didymellaceae, this followed by the separation of *Neodidymelliopsis* and *Xenodidymella* in the late Oligocene. Other 23 genera diverged from others repeatedly in the Miocene. We speculate that geological changes such as mountain uplift, climate changes and aridification in the Miocene which led to an expansion of plants, might have resulted in the emergence of plant associated fungi as in Didymellaceae genera (Aveskamp et al. 2008, Chen et al. 2015). Iranian *Neodidymelliopsis* sp. and *Didymella* sp. isolates diverged from other isolates in the Pliocene and the late Miocene, respectively (Supplementary table 5), before switching to more seasonal, drier and cooler climate (Amo De Paz et al. 2011).

Moreover, the crown ages of five genera of Didymellaceae including Iranian *Neodidymelliopsis* sp. are in the Pleistocene. This result suggests that the glaciation event of Pleistocene is not restrictive for these genera, as already proposed for some *Melanohalea* species (Ascomycetes) by Leavitt et al. (2012). Five genera including *Ascochyta*, *Neoascochyta*, *Heterophoma*, *Phomatodes* and *Neomicrosphaeropsis* are specific to Fabaceae (Rosids), Poaceae (Monocots), Scrophulariaceae (Asterids), Brassicaceae (Rosids) and Tamaricaceae (Asterids), respectively. Among these five genera, *Neoascochyta* is the oldest genus which is hosted by Monocots which are older than Asterids and Rosids (Barba-Montoya et al. 2018). The estimated ages of *Ascochyta* and *Phomatodes* chronologically corresponds to the age of their hosts *viz*. Fabaceae and Brassicaceae, estimated by Hohmann et al. (2015). This coincidence supports the co-evolution of Didymellaceae and their host plants proposed by Chen et al. (2017).

Furthermore, we compared the crown ages of *Aigialus*, Capnodiales and Didymellaceae with previous studies (Supplementary table 3). In agreement with Phukhamsakda et al. (2016), we dated *Aigialus* and Capnodiales to Eocene and Cretaceous, respectively. Similar to Prieto & Wedin (2013) study, we dated the Dothideomycetes crown group to the late Jurassic or early Cretaceous. The variation in the ages of the taxa in previous studies could be the consequence of using different fossils, models, sampling and characters. Additionally, previous studies have mostly used a controversial fossil of *Paleopyrenomycetes* to calibrate nodes of the tree (Prieto & Wedin 2013, Beimforde et al. 2014). Higher estimated ages in other studies can also be the result of considering exponential or normal distribution as the prior distribution for secondary calibration on the root note. In contrary, we prefer to use a uniform distribution, which based on Schenk (2016) simulation research. Further molecular dating studies in different locations and on various fungal taxa are needed to clarify this.

Acknowledgements

Partial financial support for this work by a research grant (No. 32−996) from the Research Council of Bu-Ali Sina University, Hamedan, Iran, is gratefully acknowledged.

References

Amo de Paz G, Cubas P, Divakar PK, Lumbsch HT, Crespo A. 2011 – Origin and Diversification of Major Clades in Parmelioid Lichens (Parmeliaceae, Ascomycota) during the Paleogene Inferred by Bayesian Analysis. PLoS One.

Aveskamp MM, de Gruyter J, Woudenberg JHC, Verkley G, Crous PW. 2010 – Highlights of the Didymellaceae: a polyphasic approach to characterise Phoma and related pleosporalean genera. Studies in Mycology 65, 1–60.

Aveskamp MM, de Gruyter J, Crous PW. 2008 – Biology and recent developments in the systematics of *Phoma*: a complex genus of major quarantine significance. Fungal Diversity 31, 1–18.

Barba-Montoya J, dos Reis M, Schneider H, Donoghue PCJ, Yang Z. 2018 – Constraining uncertainty in the timescale of angiosperm evolution and the veracity of a Cretaceous Terrestrial Revolution. New Phytologist 218, 819–834.

Beimforde C, Feldberg K, Nylinder S, Rikkinen J et al. 2014 – Estimating the Phanerozoic history of the Ascomycota lineages: combining fossil and molecular data. Molecular Phylogenetics and Evolution 78, 386–398.

Berbee M, Taylor JW. 2010 – Dating the molecular clock in fungi-how close are we? Fungal Biology Reviews 24, 1–16.

Boehm EW, Mugambi GK, Miller AN, Huhndorf SM et al. 2009 – A molecular phylogenetic reappraisal of the Hysteriaceae, Mytilinidiaceae and Gloniaceae (Pleosporomycetidae, Dothideomycetes) with keys to world species. Studies in Mycology 64, 49–83.

Chen Q, Hou LW, Duan WJ, Crous PW, Cai L. 2017 – Didymellaceae revised. Studies in Mycology 87, 105–156.

Chen Q, Jiang JR, Zhang GZ, Cai L, Crous PW. 2015 – Resolving of *Phoma enigma*. Studies in Mycology 82, 137–217.

Chomnunti P, Hongsanan S, Hudson BA, Tian Q et al. 2014 – The sooty moulds. Fungal Diversity 66, 1–36.

Crous PW, Gams W, Stalpers JA, Vincent R. et al. 2004 – MycoBank: an online initiative to launch mycology into the 21st century. Studies in Mycology 50, 19–22.

Crous PW, Groenewald JZ. 2017 – The Genera of Fungi – G 4: *Camarosporium* and *Dothiora*. IMA Fungus 8, 131–152.

Dai DQ, Boonmee S, Tian Q, Xiao YP et al. 2014 – Englerulaceae (Dothideomycetes). Phytotaxa 176(1), 139–155.

de Gruyter J, Aveskamp MM, Woudenberg JHC, Verkley GJM et al. 2009 – Molecular phylogeny of *Phoma* and allied anamorph genera: Towards a reclassification of the *Phoma* complex. Mycological Research 113, 508–519.

de Hoog GS, Gerrits van den EAHG. 1998 – Molecular diagnostics of clinical strains of filamentous Basidiomycetes. Mycoses 41, 183–189.

dos Reis M, Donoghue PCJ, Yang Z. 2015 – Bayesian molecular clock dating of species divergences in the genomics era. Nature Reviews Genetics 17, 71–80.

Doyle JJ, Doyle JL. 1987 – A rapid DNA isolation procedure for small quantities of fresh leaf tissue. Phytochemical Bulletin 19, 11–15.

Drummond AJ, Bouckaert RR. 2014 – Bayesian evolutionary analysis with BEAST 2. Cambridge University Press.

Drummond AJ, Suchard MA, Xie D, Rambaut A. 2012 – Bayesian Phylogenetics with BEAUti and the BEAST 1.7. Molecular Biology and Evolution 29 (8), 1969–73.

Ferreira MAR, Suchard MA. 2008 – Bayesian analysis of elapsed times in continuous-time Markov chains. Canadian Journal of Statistics 36 (3), 355–368.

Gueidan C, Ruibal C, de Hoog S, Schneider H. 2011 – Rock-inhabiting Fungi originated during periods of dry climate in the late Devonian and middle Triassic. Fungal Biology 115, 987–996.

Hashimoto A, Matsumura M, Hirayama K, Fujimoto R et al. 2017 – Pseudodidymellaceae fam. nov.: phylogenetic affiliations of mycopappus-like genera in Dothideomycetes. Studies in Mycology 87, 187–206.

Ho SYW, Duchene S. 2014 – Molecular-clock methods for estimating evolutionary rates and timescales. Molecular Ecology 23 (24), 5947–5965.

Ho SYW, Philips MJ. 2009 – Accounting for calibration uncertainty in phylogenetics estimation of evolutionary divergence time. Systematic Biology 58(3), 367–380.

Hohmann N, Wolf EM, Lysak MA, Kocha MA. 2015 – A Time-Calibrated Road Map of Brassicaceae Species Radiation and Evolutionary History. The Plant Cell 27, 2770–2784.
Hongsanan S, Sánchez-Ramírez S, Crous PW, Ariyawansa HA et al. 2016 – The evolution of fungal epiphytes. Mycosphere 7, 1690–1712.
Hyde KD, Hongsanan S, Jeewon R, Bhat DJ et al. 2016 – Fungal diversity notes 367–490: taxonomic and phylogenetic contributions to fungal taxa. Fungal Diversity 80, 1–270.
Hyde KD, Maharachchikumbura SSN, Hongsanan S, Samarakoon MC et al. 2017 – The ranking of fungi—a tribute to David L. Hawksworth on his 70th birthday. Fungal Diversity 84, 1–23.
Hyde KD, Nilsson RH, Alias SA, Ariyawansa HA et al. 2014 – One stop shop: backbones trees for important phytopathogenic genera: I. Fungal Diversity 67, 21–125.
Jia F, Lo N, Ho YW. 2014 – The impact of modelling rate heterogeneity among sites on phylogenetic estimates of intraspecific evolutionary rates and timescales. Plos One 9(5), e95722.
Katoh K, Standley DM. 2013 – MAFFT multiple sequence alignment software version 7: Improvements in performance and usability. Molecular Biology and Evolution 30, 772–780.
Kirk PM, Cannon PF, Minter DW, Stalpers JA. 2008 – Dictionary of the Fungi. Tenth Edition CSIRO.
Leavitt SD, Esslinger TL, Divakar PK Lumbsch HT. 2012 – Miocene and Pliocene dominated diversification of the lichen-forming fungal genus Melanohalea (Parmeliaceae, Ascomycota) and Pleistocene population expansions. Evolutionary Biology 12, 176.
Liu JK, Hyde KD, Jeewon R, Phillips AJL et al. 2017 – Ranking higher taxa using divergence times: a case study in Dothideomycetes. Fungal Diversity 84, 75–99.
Liu YJ, Whelen S, Hall BD. 1999 – Phylogenetic relationships among ascomycetes: evidence from an RNA polymerase II subunit. Molecular Biology and Evolution 16, 1799–1808.
Maddison WP, Maddison DR. 2015 – Mesquite: a modular system for evolutionary analysis. Version 3.04.
Mindell RA, Stockey RA, Beard G, Currah RS. 2007 – Margaretbarromyces dictyosporus gen. sp. nov.: a permineralized corticolous ascomycete from the Eocene of Vancouver Island, British Columbia. Mycological Research 111, 680–684.
Moran RJ, Morgan CC, O'Connell MJ. – 2015 A guide to phylogenetic reconstruction using heterogeneous models—a case study from the root of the placental mammal tree. Computation, 3, 77–196.
Nguyen LT, Schmidt HA, von Haeseler A, Minh BQ. 2014 – IQ-TREE: A fast and effective stochastic algorithm for estimating maximum-likelihood phylogenies. Molecular Biology and Evolution 32 (1), 268–274.
Pérez-Ortega S, Garrido-Benavent I, Grube M, Olmo R, de los Ríos A. 2016 – Hidden diversity of marine borderline lichens and a new order of fungi: Collemopsidiales (Dothideomyceta). Fungal Diversity 80, 285–300.
Phukhamsakda C, Hongsanan S, Ryberg M, Ariyawansa HA et al. 2016 – The evolution of Massarineae with Longipedicellataceae fam. nov. Mycosphere 7 (11), 1713–1731.
Prieto M, Wedin M. 2013 – Dating the diversification of the major lineages of Ascomycota (Fungi). PLoS One 14, e65576.
Rehner SA, Samuels GJ. 1994 – Taxonomy and phylogeny of Gliocladium analysed from nuclear large subunit ribosomal DNA sequences. Mycological Research 98, 625–634.
Rutschmann F. 2006 – Molecular Dating of phylogenetic trees: a brief review of current methods that estimate divergence times. Diversity and Distributions 12 (1), 35–48.
Schenk JJ. 2016 – Consequences of Secondary Calibrations on Divergence Time Estimates. PLoS One 11(1), 1–17.
Schmidt AR, Beimforde C, Seyfullah LJ, Wege SE et al. 2014 – Amber fossils of sooty moulds. Review of Palaeobotany and Palynology 200, 53–64.

Sung GH, Sung JM, Hywel-Jones NL, Spatafor JW. 2007 – A multi-gene phylogeny of Clavicipitaceae (Ascomycota, Fungi): identification of localized incongruence using a combinational bootstrap approach. Molecular Phylogenetics and Evolution 44. 1204–1223.

Taylor JE, Hyde KD. 2003 – Microfungi of tropical and temperate palms. Fungal Diversity Research 12, 1–459.

Vaidya G, Lohman D, Meier J. 2011 – SequenceMatrix: concatenation software for the fast assembly of multi-gene datasets with character set and codon information. Cladistics 27, 171–180.

Valenzuela-Lopez N, Cano-Lira JF, Guarro J, Sutton DA et al. 2018 – Coelomycetous Dothideomycetes with emphasis on the families Cucurbitariaceae and Didymellaceae. Studies in Mycology 90, 1–69.

Vijaykrishna D, Jeewon R, Hyde KD. 2006 – Molecular taxonomy, origins and evolution of freshwater ascomycetes. Fungal Diversity 23, 351–390.

Vilgalys R, Hester M. 1990 – Rapid genetic identification and mapping of enzymatically amplified ribosomal DNA from several Cryptococcus species. Journal of Bacteriology 17, 4238–4246.

White TJ, Bruns T, Lee S, Taylor J. 1990 – Amplification and direct sequencing of fungal ribosomal RNA genes for phylogenetics. PCR Protocols: A guide to Methods and Applications.

Wijayawardene NN, Hyde KD, Dhanushka NW, Papizadeh M et al. 2016 – Taxonomy and phylogeny of dematiaceous coelomycetes. Fungal Diversity 77, 1–310.

Wijayawardene NN, Hyde KD, Lumbsch HT, Liu JK et al. 2018 – Outline of Ascomycota: 2017. Fungal Diversity 88, 167–263.

Wijayawardene NN, Hyde KD, Rajeshkumar KC, Hawksworth DL et al. 2017 – Notes for genera – Ascomycota. Fungal Diversity. 86, 1–594.

Woudenberg JHC, Aveskamp MM, de Gruyter J, Spiers AG, Crous PW. 2009 – Multiple *Didymella* teleomorphs are linked to the Phoma clematidina morphotype. Persoonia 22, 56–62.

Zhao RL, Zhou JL, Chen J, Margaritescu S et al.2016 – Towards standardizing taxonomic ranks using divergence times-a case study for reconstruction of the *Agaricus* taxonomic system. Fungal Diversity 78, 239–292.

Zuckerkandl E, Pauling L. 1965 – Evolutionary divergence and convergence in proteins. Evolving Genes and Proteins 97–166.

Supplementary Informations

Supplementary table 1 Strains used in this study and their GeneBank accession numbers.

Isolate name	Strain number	Host	Province	GeneBank Accession Number			
				LSU	TUB	RPB2	ITS
IR26	CBS 142211; IRAN 2770C	*Citrus paradisi*	Khuzestan	KY355074	KY407790	KY386285	KY290226
IR14	CBS 142210;	*Citrus aurantium*	Kerman	KY355073	KY407789	KY386284	KY290225
IR10	CBS 142208; IRAN 2771C	*Citrus sinensis*	Kerman	KY355072	KY407788	KY386283	KY290224
IR67	CBS 142212 IRAN 2768C	*Citrus lemon*	Hormozgan	KY355075	KY407791	KY386286	KY290228

Supplementary table 2 GeneBank, culture collection code and accession numbers of the isolates used in this study.

Species Name	Strain Number[1]	Host, Substrate	Country	GeneBank Accession Number			
				LSU	ITS	TUB	RPB2
Aigialus grandis	BCC 20000	Mangrove wood	Malaysia	GU479775	-	-	GU479814
A. mangrovei	BCC 33563	Mangrove wood	Thailand	GU479776	-	-	GU479815
A. parvus	BCC 18403	Mangrove wood	Malaysia	GU479778	-	-	GU479817
A. rhizophorae	BCC 33572	Mangrove wood	Thailand	GU479780	-	-	GU479819
Allophoma labilis	CBS 124.93	*Solanum lycopersicum*	The Netherlands	GU238091	GU237765	GU237619	KT389552
A. minor	CBS 325.82; FMR 14905	*Syzygium aromaticum*	Indonesia	GU238107	GU237831	GU237632	KT389553
A. piperis	CBS 268.93	*Peperomia pereskiifolia*	The Netherlands	GU238129	GU237816	GU237644	KT389554
A. zantedeschiae	CBS 131.93	*Calla* sp.	The Netherlands	GU238159	FJ427084	FJ427188	KT389557
Ascochyta rabiei	CBS 206.30	Unknown	Unknown	KT389695	KT389478	KT389772	KT389559
A. versabilis	CBS 876.97	*Silene* sp.	The Netherlands	GU238152	GU237909	GU237664	KT389561
A. viciae	CBS 451.68	*Vicia sepium*	The Netherlands	KT389701	KT389484	KT389778	KT389562
Boeremia exigua1	CBS 118.38	*Cheiranthus cheiri*	Denmark	KT389706	KT389489	KT389783	KT389582
B. exigua2	CBS 119.38	*Nicotiana tabacum*	Unknown	KT389707	KT389490	KT389784	KT389583
B. lycopersici	CBS 378.67	*Solanum lycopersicum*	The Netherlands	GU237950	GU237848	GU237512	KT389580
Briansuttonomyces eucalypti	CBS 114879; CPC 362	*Eucalyptus* sp.	South Africa	KU728519	KU728479	KU728595	-
B. eucalypti	CBS 11887; CPC 363	*Eucalyptus* sp.	South Africa	KU728520	KU728480	KU728596	-
Calophoma. aquilegiicola	CBS 107.96	*Aconitum pyramidale*	The Netherlands	GU238041	GU237735	GU237581	KT389586
C. clematidina	CBS 102.66	*Clematis* sp.	UK	FJ515630	FJ426988	FJ427099	KT389587
C. clematidis-rectae	CBS 507.63	*Clematis* sp.	The Netherlands	FJ515647	FJ515606	FJ515624	KT389589
C. rosae	CGMCC 3.18347	*Rosa* sp.	China	KY742203	KY742049	KY742291	KY742135
Capnodiales sp.001	010301	*Dacrydium araucarioides*	New Caledonia	KF157991	-	-	-
Capnodiales sp.003	010302	*Epiphytic fungus*	New Caledonia	KF157992	-	-	-
Capnodium coffeae	CBS 147.52			DQ247800	-	-	DQ247788
Cumuliphoma indica1	CBS 654.77; FMR 15341	Unknown	India	GU238122	FJ427043	FJ427153	LT623261
C.indica2	CBS 991.95; FMR 15331	Soil	Papua New Guinea	GU238121	FJ427044	FJ427154	LT623262

Supplementary table 2 Continued.

Species Name	Strain Number[1]	Host, Substrate	Country	GeneBank Accession Number			
				LSU	ITS	TUB	RPB2
C. omnivirens	CBS 341.86; FMR 14915	*Phaseolus vulgaris*	Belgium	LT623214	FJ427042	FJ427152	LT623260
C. pneumoniae	CBS 142454; UTHSC: DL16-246; FMR 13739	Human respiratory tract	USA	LN907392	LT592925	LT592994	LT593063
D. aliena	CBS 379.93	*Berberis* sp.	TheNetherlands	GU238037	GU237851	GU237578	KP330416
D. arachidicola	CBS 333.75	*Arachis hypogaea*	South Africa	GU237996	GU237833	GU237554	KT389598
D. glomerata	CBS 528.66; PD 63/590	*Chrysanthemum* sp.	TheNetherlands	JX681105	FJ427013	FJ427124	GU371781
Didymella pinodes	CBS 525.77	*Pisum sativum*	Belgium	GU238023	GU237883	GU237572	KT389614
Ectophoma multirostrata1	CBS 110.79; FMR 15342	*Cucumis sativus*	TheNetherland	GU238110	FJ427030	FJ427140	LT623264
E. multirostrata2	CBS 274.60; FMR 15335	Soil	Maharashtra	GU238111	FJ427031	FJ427141	LT623265
E. multirostrata3	CBS 368.65; FMR 15336	Unknown	India	GU238112	FJ427033	FJ42714 3L	T623266
E. pomi	CBS 267.92; FMR 15346	*Coffea arabica*	India	GU238128	GU237814	GU237643	LT623263
Epicoccum brasiliense	CBS 120105; FMR 14907	*Amaranthus* sp.	Brazil	GU238049	GU237760	GU237588	KT389627
E. draconis	CBS 186.83; FMR14908	*Dracaena* sp.	Rwanda	GU238070	GU237795	GU237607	KT389628
E. henningsii	CBS 104.80	*Acaciamearnsii*	Kenya	GU238081	GU237731	GU237612	KT389629
E. plurivorum	CBS 558.81; FMR 14909	*Setaria* sp.	New Zealand	GU238132	GU237888	GU237647	KT389634
Heterophoma adonidis	CBS 114309	*Adonis vernalis*	Sweden	KT389724	KT389506	KT389803	KT389637
H. nobilis	CBS 507.91	*Dictamnus albus*	The Netherlands	GU238065	GU237877	GU237603	KT389638
H. verbascicola1	CGMCC 3.18364	*Verbascum thapsus*	China	KY742273	KY742119	KY742361	KY742187
H. verbascicola2	LC 8164	*Verbascum thapsus*	China	KY742274	KY742120	KY742362	KY742188
Juxtiphoma eupyrena1	CBS 374.91; FMR 15329	*Solanum tuberosum*	The Netherlands	GU238072	FJ426999	FJ427110	LT623268
J. eupyrena2	CBS 527.66; FMR 15337	Wheat field soil	Germany	GU238073	FJ427000	FJ427111	LT623269
Leptosphaerulina americana	CBS 213.55	*Trifolium pratense*	USA	GU237981	GU237799	GU237539	KT389641
L. australis	CBS 317.83	*Eugenia aromatica*	Indonesia	EU754166	GU237829	GU237540	GU371790
Macroventuria anomochaeta	CBS 525.71	*Decayed canvas*	South Africa	GU237984	GU237881	GU237544	GU456346
M. wentii	CBS 526.71	*Plant litter*	USA	GU237986	GU237884	GU237546	KT389642
Neoascochyta desmazieri	CBS 297.69	*Lolium perenne*	Germany	KT389726	KT389508	KT389807	KT389644

Supplementary table 2 Continued.

Species Name	Strain Number[1]	Host, Substrate	Country	GeneBank Accession Number			
				LSU	ITS	TUB	RPB2
N. europaea	CBS 820.84	*Hordeum vulgare*	Germany	KT389729	KT389511	KT389809	KT389646
N. exitialis	CBS 118.40	Unknown	Unknown	KT389732	KT389514	KT389812	KT389647
N. graminicola	CBS 301.69	*Lolium multiflorum*	Germany	KT389737	KT389519	KT389817	KT389650
Neodidymelliopsis cannabis	CBS 234.37	*Cannabis sativa*	Unknown	GU237961	GU237804	GU237523	KP330403
N. longicolla	CBS 38296	Soil in desert	Israel	KT389750	KT389532	KT389830	-
N. polemonii	CBS 109181	*Polemonium caeruleum*	TheNetherlands	GU238133	GU237746	KT389828	KP330427
N. xanthina	CBS 383.68	*Delphinium* sp.	TheNetherlands	GU238157	GU237855	KT389831	KP330431
Neomicrosphaeriopsis italica	MFLUCC 15-0485	*Tamarix* sp.	Italy	KU729854	KU900318	-	KU674820
N. italica	MFLUCC 15-0484	*Tamarix* sp.	Italy	KU729853	KU900319	KX453298	KU695539
Nothophoma anigozanthi	CBS 381.91; FMR 14914	*Anigozanthus maugleisii*	The Netherlands	GU238039	GU237852	GU237580	KT389655
N. arachidis-hypogaeae	CBS 125.93	*Arachis hypogaea*	India	GU238043	GU237771	GU237583	KT389656
N. gossypiicola	CBS 377.67; FMR14912	*Gossypium* sp.	USA	GU238079	GU237845	GU237611	KT389658
N. infossa	CBS 123395	*Fraxinus pennsylvanica*	Argentina	GU238089	FJ427025	FJ427135	KT389659
Paraboeremia adianticola	CBS 187.83; FMR 15344	*Polystichum adiantiforme*	USA	GU238035	GU237796	GU237576	KP330401
P. litseae	CGMCC 3.18110	*Litsea* sp.	China	KX829037	KX829029	KX829053	KX829045
P. putaminum	CBS 130.69; FMR 15338	*Malus sylvestris*	Denmark	GU238138	GU237777	GU237652	LT623254
P. selaginellae	CBS122.93	*Selaginella* sp.	The Netherlands	GU238142	GU237762	GU237656	LT623255
Phoma herbarum1	CBS 377.92; IMI 21384	Human leg	UK	KT389756	KT389536	KT389837	KT389663
P. herbarum2	UTHSC:DL16-319; FMR 13812	*Humansuperficial tissue*	USA	LN907462	LT592955	LT593024	LT593024
P. herbarum3	CBS 502.91	*Nerium* sp.	The Netherlands	GU238082	GU237874	GU237613	KP330419
P. herbarum4	CBS 615.75; FMR 15340	*Rosa multiflora* cv. *Cathayensis*	The Netherlands	KF251715	FJ427022	KF252703	KP330420
Phomatodes aubrietiae	CBS 627.97	*Aubrietia* sp.	The Netherlands	GU238045	GU237895	GU237585	KT389665
P. nebulosi	CBS 100191	*Thlaspi arvense*	Poland	KP330446	KP330434	KP330390	KT389666
P. nebulosi	CBS 740.96	*Armoracia rusticana*	The Netherlands	KT389758	KT389540	KT389839	KT389667
Pseudoascochyta novae-zelandiea	CBS 141689; FMR 15110; ICMP 10493	*Cordyline australis*	New Zealand	LT592893	LT592892	LT592894	LT592895

Supplementary table 2 Continued.

Species Name	Strain Number[1]	Host, Substrate	Country	GeneBank Accession Number			
				LSU	ITS	TUB	RPB2
P. pratensis	CBS 141688; FMR 14524	Soil	Spain	LT223131	LT223130	LT223132	LT223133
Remotididymella anthropophila	CBS 142462; UTHSC:DI16-278; FMR 13770	Human respiratory tract	USA	LN907421	LT592936	LT593005	LT593075
R. destructiva1	CBS 133.93; FMR 15349	*Solanum lycopersicon*	Guadeloupe	GU238064	GU237779	GU237602	LT623257
R. destructiva2	CBS 378.73; FMR 15328	*Lycopersicon esculentum*	Tonga	GU238063	GU237849	GU237601	LT623258
R. destructiva3	CBS 162.78; FMR 14906	*Lycopersicon esculentum*	The Netherlands	GU238062	GU237788	GU237600	LT623259
Similiphoma crystallifera	CBS 193.82; FMR 1534	*Chamaespartium sagittale*	Austria	GU238060	GU237797	GU237598	LT623267
Stagonosporopsis dorenboschii	CBS 426.90	*Physostegia virginiana*	The Netherlands	GU238185	GU237862	GU237690	KT389678
S. hortensis	CBS 572.85	*Phaseolus vulgaris*	The Netherlands	GU238199	GU237893	GU237704	KT389681
Vacuiphoma bulgarica	CBS 357.84; FMR 14917	*Trachystemon orientale*	Bulgaria	GU238050	GU237837	GU237589	LT623256
V. oculihominis	UTHSC:DI16-308; FMR 13801	*Human superficial tissue*	USA	LN907451	LT592954	LT593023	LT593093
Xenodidymella applanata	CBS 205.63	*Rubus idaeus*	The Netherland	GU237998	GU237798	GU237556	KP330402
X. asphodeli	CBS 375.62	*Asphodelus albus*	France	KT389765	KT389549	KT389853	KT389689
X. catariae	CBS 102635	*Nepeta catenaria*	The Netherlands	GU237962	GU237727	GU237524	KP330404
X. humicola	CBS 220.85	*Franseria* sp.	USA	GU238086	GU237800	GU237617	KP330422

1 Abbreviation of culture collections: CBS: Centraalbureau voor Schimmelcultures, Utrecht, The Netherlands; CGMCC: China General Microbiological Culture Collection, Beijing, China; CPC: Culture collection of Pedro Crous, housed at CBS; FMR, Facultatde Medicina, Universitat Rovirai Virgili, Reus, Spain; ICMP: International Collection of Microorganisms from Plants, Auckland, New Zealand; IMI: International Mycological Institute, CABI-Bioscience, Egham, Bakeham Lane, IRAN: Iranian Fungal Culture Collection, Iranian Research Institute of Plant Protection, Iran; U.K.; LC: Cultur collection of Qian Chen, housed at CAS, China; MFLUCC: Mae Fah Luang University Culture Collection, Chiang Rai, Thailand; PD: Plant Protection Service, Wageningen, the Netherlands; UTHSC, Fungus Testing Laboratory at the University of Texas Health Science Center, San Antonio, Texas, USA.

Supplementary table 3 The divergence time of the nodes in different study

Node	This study	Beimforde et al. (2014)	Prieto & Wedin (2013)	Gueidan et al. (2011)	Phukhamsakda et al. (2016)	Pérez-Ortega et al. (2016)
DOT	144.5 (107-202.9)	350 (273–459	174 (107-204)	338	293 (213-371)	290
DID	35.7 (18.4-63.5)	-	-	-	-	-

Supplementary table 3

Node	This study	Beimforde et al. (2014)	Prieto & Wedin (2013)	Gueidan et al. (2011)	Phukhamsakda et al. (2016)	Pérez-Ortega et al. (2016)
PLE	86.7 (53.9-155.4)	-	-	-	211 (153-277)	-
CAP	99 (99-100)	-	-	-	147 (102-202)	-
AIG	34.1 (34-64.4)	-	-	-	39 (35-49)	-

Supplementary table 4 Time chart of the nodes based on the estimated crown age in the current study*

Period	Epoch	Stage	Age	Taxa
Quaternary	Holocene		0-0.012	
	Pleistocene	Late	0.012-0.126	***Briansuttonomyces***
		Middle	0.126-1.8	*Neomicrosphaeropsis;* *Phoma;* *Juxtiphoma;* Iranian *Neodidymelliopsis;* *Pseudoascochyta*
		Early	1.8-2.58	-
	Miocene	Late	5.33-11.63	*Paraboeremia;* *Leptosphaerulina;* *Allophoma;* *Ascochyta;* *Heterophoma;* *Stagonosporopsis;* *Epicoccum;* *Remotididymella;* *Vacuiphoma;* *Nothophoma;* *Neodidymelliopsis*;
		Middle	11.63-16	*Calophoma;* *Didymella;* *Neoascochyta;* *Similiphoma;* ***Xenodidymella*;**
		Early	16-23.03	-
Paleogene	Oligocene	Late	23.03-27.82	-
		Early	27.82-33.9	
	Eocene	Late	33.9-37.8	*Aigialus*; Didymellaceae
		Middle	37.8-47.8	
		Early	47.8-56	
	Paleocene		56-66	
Cretaceous			66-147.5	Pleosporales; Capnodiales; Dothideomycetes

*The geological time scales were retrieved from the International Commission on Stratigraphy (ICS) website (www.stratigraphy.com)

Supplementary table 5 Time chart of the nodes based on the estimated stem age in the current study*

Period	Epoch	Stage	Age	Taxa
Quaternary	Holocene		0-0.012	
	Pleistocene	Late	0.012-2.58	-
Neogene	Pliocene		2.58-5.33	Iranian *Neodidymelliopsis*- *Neodidymelliopsis*
	Miocene	Late	5.33-11.63	*Briansuttonomyces* *Pseudoascochyta* Iranian *Didymella*- *Didymella* *Allophoma* *Heterophoma* *Ascochyta* *Phomatodes*
		Early	16-23.03	*Remotididymella* *Phoma* *Similiphoma* *Macroventuria* *Didymella* *Nothophoma* *Calophoma* *Juxtiphoma* *Leptosphaerulina* *Vacuiphoma*
Paleogene	Oligocene	Late	23.03-27.82	*Xenodidymella* *Neodidymelliopsis*
		Early	27.82-33.9	-
	Eocene	Late	33.9-37.8	*Neoascochyta*
		Middle	37.8-47.8	-
		Early	47.8-56	-
	Paleocene		56-66	
Cretaceous			66-147.5	*Aigialus*- Didymellaceae Pleosporales- Capnodiales

*The geological time scales were retrieved from the International Commission on Stratigraphy (ICS) website (www.stratigraphy.com)

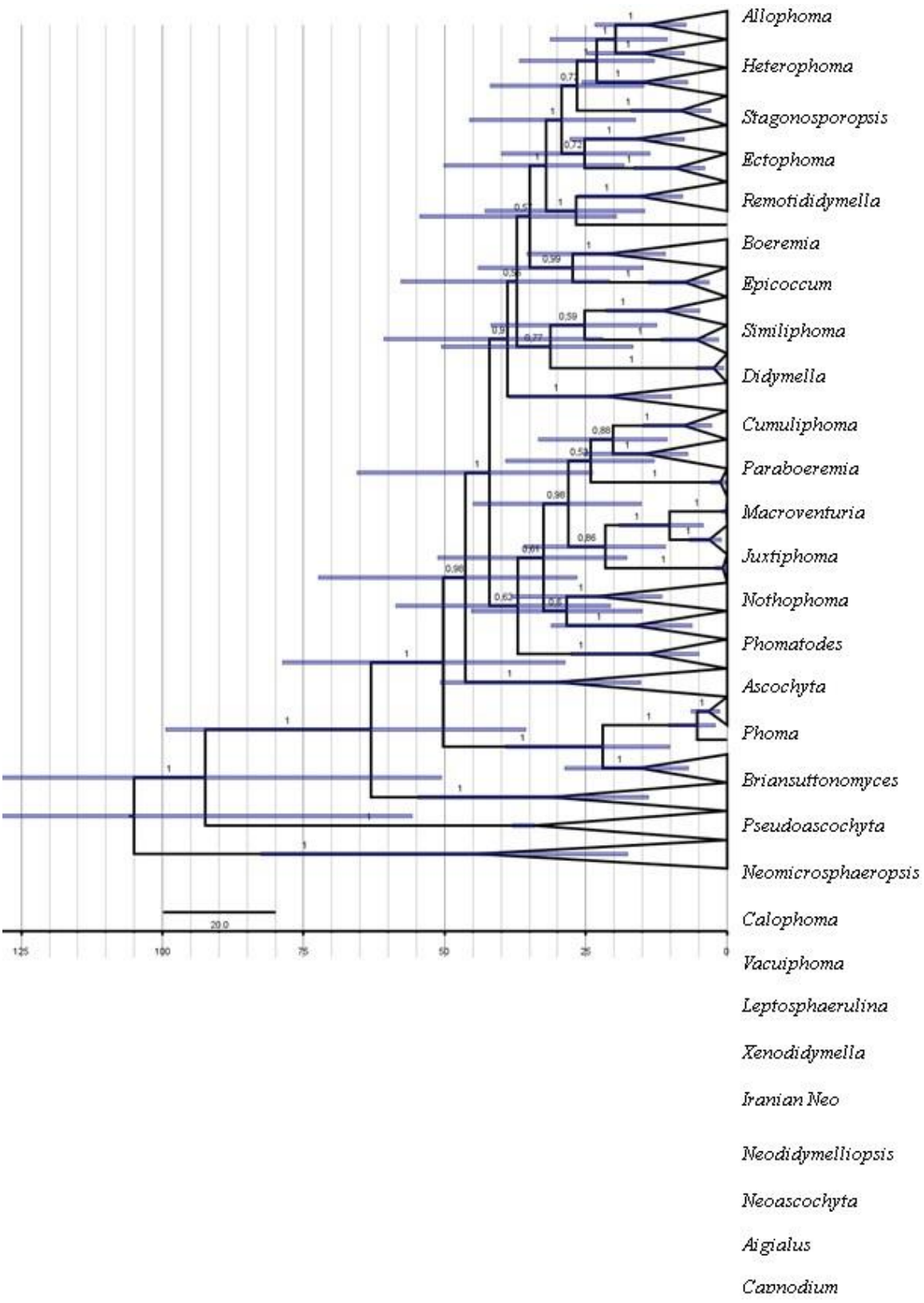

Supplementary figure 1 – Dated phylogenetic tree of scenario I. The numbers next to the nodes indicate posterior probability values.

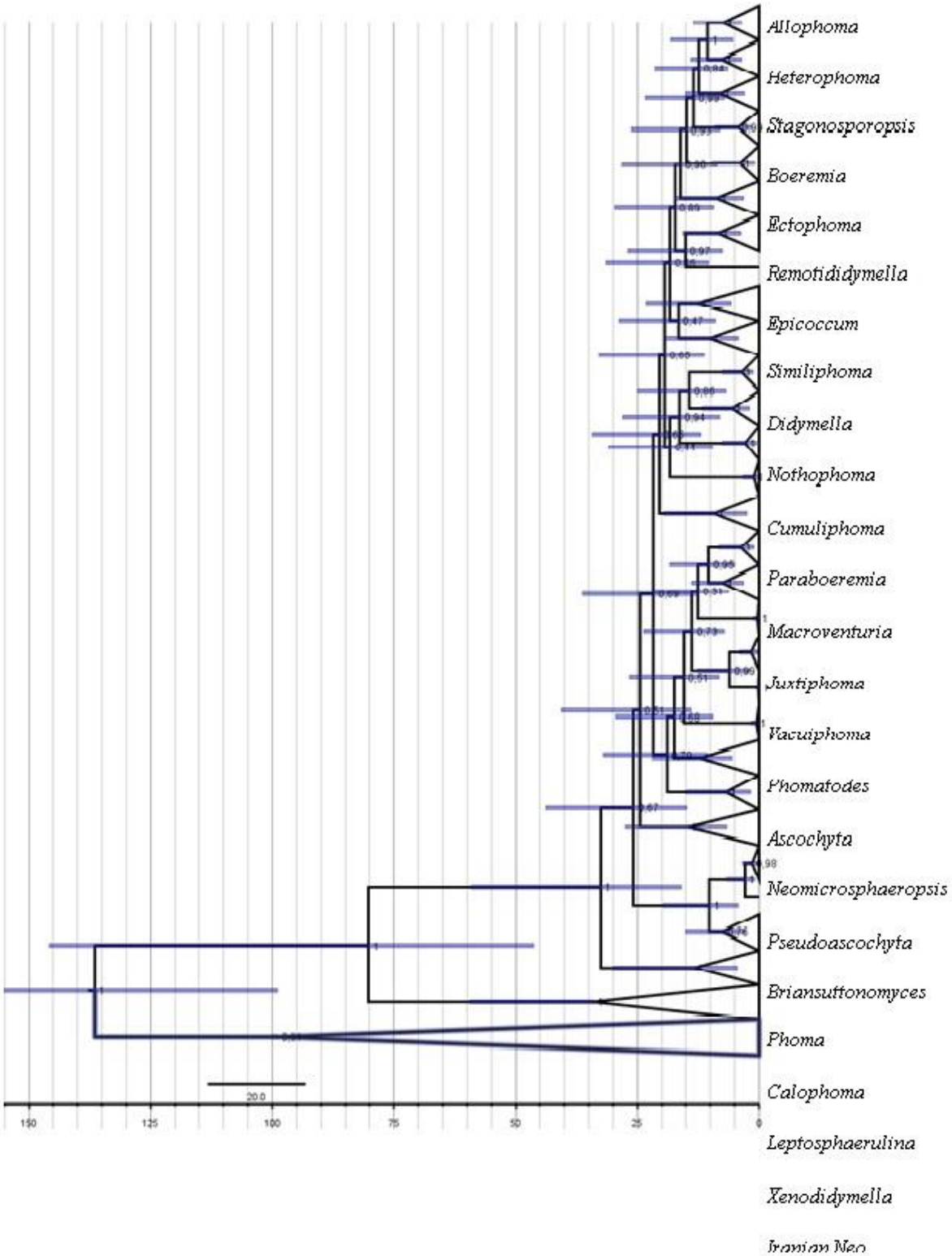

Supplementary figure 2 – Dated phylogenetic tree of scenario II. The numbers next to the nodes indicate posterior probability values.

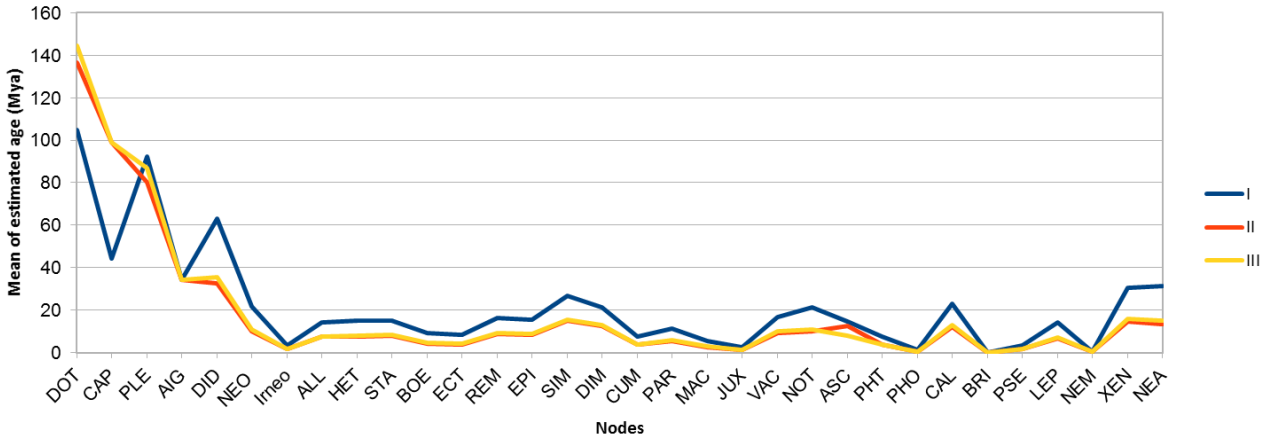

Supplementary figure 3 – The means of estimated age of different nodes in scenario I (blue), II (red) and III (yellow)